



Contents lists available at ScienceDirect

Physics Letters A

www.elsevier.com/locate/pla



# Topological dependence of Kepler's third law for collisionless periodic three-body orbits with vanishing angular momentum and equal masses

V. Dmitrašinović\*, Milovan Šuvakov

*Institute of Physics, Belgrade University, Pregrevica 118, Zemun, P.O.Box 57, 11080 Beograd, Serbia*

## ARTICLE INFO

### Article history:

Received 14 April 2015

Received in revised form 10 June 2015

Accepted 11 June 2015

Available online xxxx

Communicated by C.R. Doering

### Keywords:

Celestial mechanics

Three-body systems in Newtonian gravity

Nonlinear dynamics

## ABSTRACT

We present results of numerical calculations showing a three-body orbit's period's  $T$  dependence on its topology. This dependence is a simple linear one, when expressed in terms of appropriate variables, suggesting an exact mathematical law. This is the first known relation between topological and kinematical properties of three-body systems. We have used these results to predict the periods of several sets of as yet undiscovered orbits, but the relation also indicates that the number of periodic three-body orbits with periods shorter than any finite number is countable.

© 2015 Elsevier B.V. All rights reserved.

## 1. Introduction

There is, at present, no deeper understanding of periodic three-body orbits in Newtonian gravity, than the simple change of scale of spatial and temporal coordinates, see Section 10 of Ref. [1], that can be compared with Kepler's third law for two-body motion, Ref. [1]. Kepler extracted his laws from the astronomical data concerning two-body periodic orbits collected by Tycho Brahe and his predecessors.

Unlike a two-body orbit, a periodic three-body orbit is characterized both by its kinematic and geometric properties and by its topology, which can be described algebraically by a word, or an element  $w(a, b, A, B)$  of free group  $F_2$  on two letters  $a, b$  (and their inverses  $A = a^{-1}$ ,  $B = b^{-1}$ ), see Refs. [2–4]. The algorithm used for “reading” of words corresponding to periodic orbits is described in the Appendix of Ref. [4].

Graphically, this amounts to classifying closed curves according to their “topologies” in a plane with two punctures. The closed curves are stereographic projections of periodic orbits from the shape-sphere, with three punctures – for a detailed explanation, see Refs. [2–4], and for graphic illustrations, see the web-site [16] – onto a plane with two punctures, the puncture at the “north pole” having been projected to infinity.

That procedure leads to the aforementioned free group  $F_2$  on two letters  $(a, b)$ , where (for definiteness)  $a$  denotes a clockwise “full turn” around the right-hand-side puncture, and  $b$  denotes the counter-clockwise full turn around the other puncture in the plane/sphere. In this way the topology of an orbit can be transformed into an algebraic object that can be further manipulated.

But, even within this particular method of assigning a sequence of symbols to a topology there remains an ambiguity, regarding the question which puncture should be taken as the “north pole” of the stereographic projection, see Appendix A.1. The length of the word generally depends on this choice, see Appendix B.1. We resolve this ambiguity by using the (common) symmetry axis of all presently known collisionless zero-angular-momentum periodic orbits to define the “north pole”, which we call the “natural”, or “symmetric” choice, because it leads to equal numbers  $n_a = n_b = \frac{1}{2}n_w$  of small letters  $a$  and  $b$ , as well as equal numbers  $n_A = n_B = \frac{1}{2}n_w$  of capital letters  $A$ , or  $B$ . These relations need not hold with a different choice of “north pole”, however, e.g. with cyclically permuted punctures, generally  $n_{1a} \neq n_{1b}$  and  $n_{1A} \neq n_{1B}$ , see Appendix B.1. Moreover, the above-described procedure, is not the only way of assigning a sequence of symbols to a topology, for an alternative, together with our results expressed in these alternative terms, see Appendix B.2.

To date there is no collection of astronomical data regarding periodic orbits of three bodies comparable to Brahe's collection of two-body orbits. Therefore, if one wishes to study general properties of the three-body system one must resort to numerical

\* Corresponding author.

E-mail address: dmitrasin@ipb.ac.rs (V. Dmitrašinović).

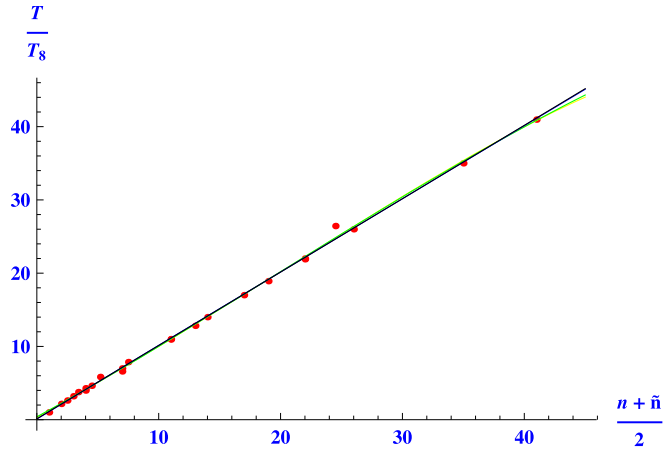


**Fig. 1.** (Color on line.) The rescaled periods  $T_r(w)$  of presently known (zero-angular-momentum) three-body orbits divided by the period of the figure-8 orbit  $T_r(w_8)$ , versus one half of the length of word  $N_w$ , i.e., one half of the number of all letters in the free-group word  $w$  describing the orbit,  $N_w/2 = (n_w + \bar{n}_w)/2$ , where  $n_w$  is the number of small letters  $a$ , or  $b$ , and  $\bar{n}_w$  is the number of capital letters  $A$ , or  $B$  in the letter  $w$ . Four (linear, quadratic, cubic and quartic) fits are shown as solid lines of different colors, yet they overlap so much that the difference can be seen only at  $N_w > 80$ .

studies. To this end, in this Letter we use the world's total (published) data set containing 46 distinct collisionless periodic orbits, Refs. [3,5–8,16], to extract the following (wholly unexpected) linear dependence of the (generalized) Kepler's third law for the ratio  $T_r(w)/T_r(w_8)$  of “rescaled” periods (i.e. periods evaluated at one common energy  $E$ ) of three-body orbits,

$$\frac{T_r(w)}{T_r(w_8)} = \frac{T_E(w)|E(w)|^{3/2}}{T_E(w_8)|E(w_8)|^{3/2}} \simeq \frac{N_w}{2} = \frac{(n_w + \bar{n}_w)}{2} \quad (1)$$

on their topologies  $w$ , specifically on (one half of) the number of all letters  $N_w = (n_w + \bar{n}_w)$ , see Fig. 1. Here  $n_w$  is the number of small letters  $a$ , or  $b$ , and  $\bar{n}_w$  is the number of capital letters  $A$ , or  $B$  contained in the latter  $w$ , and  $w_8 = abAB$  if the free-group word describing the figure-8 orbit, Refs. [2,3,5]. We have divided the total number of letters  $N_w$  into two parts because orbits fall into different classes with distinct values of  $n_w$  and  $\bar{n}_w$ , see Table 1.

The worst-case disagreement of this linear dependence with the data is about 10%, though generally it is (much) better, occasionally reaching the limits (six significant decimal places) of our numerical precision. In this Letter we point out four more accurate (than 10%), yet still approximate sub-sequences of orbits, and one possibly exact regularity. For clarity's sake, we show in Fig. 2 the corresponding graph for non-satellite orbits, only. Note that the range of the abscissa in Fig. 2 only reaches the value  $N_w = 49$ .

At this point a few words must be said about the statistical significance of results presented in Fig. 1, or equivalently about  $\#(N_w)$ , the number of distinct periodic orbits of “length”  $N_w$ : 1) At small length values one can explicitly count the mathematically allowed orbits and show that many have already been found, see Appendix A.2. 2) As one increases the number of letters  $N_w$ , the number of topologically distinct orbits  $\#(N_w)$  grows rapidly, see Appendix A.2, and the number of presently discovered (and displayed here) orbits pales in comparison with that number. The number  $\#(N_w)$  is not necessarily the same one as the number of physically possible orbits – Moore has shown by explicit examples how mathematically allowed orbits disappear as the exponent in the potential is reduced from  $a = 2$  to  $a = 1$  in Newtonian gravity, Ref. [7].

The large number of still possibly undetected orbits makes the observed linearity of the graph, Fig. 1, at higher values of  $N_w$  all

**Table 1**

Rescaled periods  $T$  of three-body orbits, their ratios with Moore's figure-8 period  $T_{M8}$ , and with period  $T_\beta$  of the first orbit  $\beta$  in the given section of the Table, as functions of the numbers  $n_a, n_b, n_A, n_B$ , of  $a$ 's,  $b$ 's,  $A = a^{-1}$ 's and  $B = b^{-1}$ 's respectively, in the free-group word description of the orbit. Note that “generic” relations  $n = n_a = n_b$  and  $\bar{n} = n_A = n_B$  hold only in the “natural” or symmetric choice of stereographic projection (see the Introduction and Appendix A.1) and that, due to the time-reversal symmetry of the solutions, the  $n$  and  $\bar{n}$  may be interchanged.

Label	$\langle T \rangle_2$	$\frac{\langle T \rangle_2}{\langle T_{M8} \rangle_2}$	$\frac{\langle T \rangle_2}{\langle T_\beta \rangle_2}$	$\frac{n+\bar{n}}{n_\beta+\bar{n}_\beta}$	$(n, \bar{n})$
M8	26.1281	1	1	1	1, 1
S8	26.1268	0.999951	0.999951	1	1, 1
I.B.1 moth I	68.4636	2.62031	1	1	2, 3
II.B.1 yarn	205.469	7.86391	3.00114	3	6, 9
IA.1 butterfly I	56.3776	2.15774	1	1	2, 2
IA.2 butterfly II	56.3746	2.15762	0.999944	1	2, 2
I.B.5 goggles	112.129	4.29152	1.9889	2	4, 4
I.B.7 dragonfly	104.005	3.98059	1	1	4, 4
IA.3 bumblebee	286.192	10.9534	2.7517	11/4	11, 11
II.C.2a yin-yang I	83.7273	3.20449	1	1	3, 3
II.C.2b yin-yang I	83.7273	3.20449	1	1	3, 3
II.C.3a yin-yang II	334.876	12.8167	3.9996	4	12, 12
II.C.3b yin-yang II	334.873	12.8166	3.9996	4	12, 12
I.B.1 moth I	68.4636	2.62031	1	1	2, 3
I.B.3 butterfly III	98.4354	3.76742	1.43778	7/5	3, 4
I.B.2 moth II	121.006	4.63126	1.76745	9/5	4, 5
I.B.4 moth III	152.33	5.83013	2.22498	11/5	5, 6
I.B.6 butterfly IV	690.627	26.4324	10.0875	49/5	24, 25

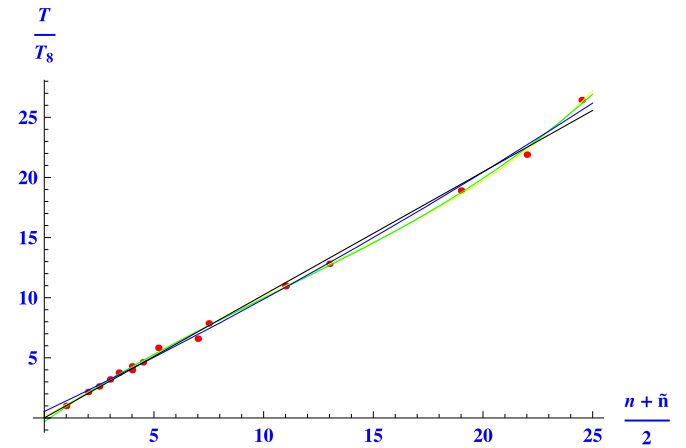


**Fig. 2.** (Color on line.) The rescaled periods  $T_r(w)$  of 16 presently known non-satellite zero-angular-momentum three-body orbits divided by the period of the figure-8 orbit  $T_r(w_8)$  versus one half of the length of word  $N_w$ , i.e., one half of the number of all letters in the free-group word  $w$  describing the orbit,  $N_w/2 = (n_w + \bar{n}_w)/2$ , where  $n_w$  is the number of small letters  $a$ , or  $b$ , and  $\bar{n}_w$  is the number of capital letters  $A$ , or  $B$  in the letter  $w$ . Four (linear, quadratic, cubic and quartic) fits are shown as solid lines of different colors.

the more impressive: Note that 24, out of grand total of 46 orbits taken from Refs. [3,5,7,8], extend up to  $N_w = 49$ . These 24 orbits include 10 (non-choreographic) figure-eight satellites from Ref. [5]. Among these 24 there are 16 non-satellite orbits that are shown separately in Fig. 2. The remaining 22 (of 46) orbits are the new ( $k = 5, 7, 14, 17, 22, 26, 35, 41$  figure-eight satellite) choreographies, Ref. [6], that extend up to  $N_w = 82$  and thus test the proposed linear dependence(s) farther into the previously unexplored region. We emphasize that three of these new choreographic orbits are not satellites of the figure-eight.

The most precise regularity explains two previously noticed, but unexplained identities: a) the identity of periods (to 16 decimal places, in Ref. [9]); and b) the identity of actions (to seven significant digits, in Ref. [10]), of two distinct orbits with the same topology, viz. of Moore's and Simo's figure-8 solutions, evaluated at equal energies. The same phenomenon was observed among seven

Download English Version:

<https://daneshyari.com/en/article/10727595>

Download Persian Version:

<https://daneshyari.com/article/10727595>

[Daneshyari.com](https://daneshyari.com)